General Disclaimer

One or more of the Following Statements may affect this Document

- This document has been reproduced from the best copy furnished by the organizational source. It is being released in the interest of making available as much information as possible.

- This document may contain data, which exceeds the sheet parameters. It was furnished in this condition by the organizational source and is the best copy available.

- This document may contain tone-on-tone or color graphs, charts and/or pictures, which have been reproduced in black and white.

- This document is paginated as submitted by the original source.

- Portions of this document are not fully legible due to the historical nature of some of the material. However, it is the best reproduction available from the original submission.

NASA

Technical Memorandum 85026

Is there any Chlorine Monoxide in the Stratosphere?

**M. J. Mumma, J. D. Rogers, T. Kostiuk,
D. Deming, and J. J. Hillman**

MAY 1983

JUN 1983
RECEIVED
NASA STI FACILITY
ACCESS DEPT.

IS THERE ANY CHLORINE MONOXIDE IN THE STRATOSPHERE?

M. J. Mumma, J. D. Rogers, T. Kostiuk, D. Deming,
J. J. Hillman

Infrared and Radio Astronomy Branch
Goddard Space Flight Center.
Greenbelt, MD 20771

D. Zipoy
Astronomy Program
University of Maryland
College Park, MD 20742

ABSTRACT

A ground-based search for stratospheric ^{35}ClO was carried out during May and October, 1981, using an infrared heterodyne spectrometer in the solar absorption mode. Lines due to stratospheric HNO_3 and tropospheric OCS were detected at about 0.2% absorptance levels, but the expected 0.1% lines of ClO in this same region were not seen. We find that stratospheric ClO is at least a factor of seven less abundant than is indicated by in situ measurements, and we set an upper limit of 2.3×10^{13} molecules cm^{-2} at the 95% confidence level for the integrated vertical column density of ClO. Our results imply that the release of chlorofluorocarbons may be significantly less important for the destruction of stratospheric ozone (O_3) than is currently thought.

Chlorofluorocarbons are important and widely used industrial chemicals, but current photochemical models of the stratosphere indicate that their release ultimately depletes the ozone layer (1). Chlorine monoxide (CℓO) is thought to be a key tracer of this process, and measurements of its stratospheric abundances are therefore particularly important. J. G. Anderson and his colleagues have reported (2) a series of in situ measurements of stratospheric CℓO, based on its chemical conversion to chlorine atoms, which are then detected by resonance fluorescence. Their results show large variations from flight-to-flight.

Since direct detection of chlorine monoxide's electronic resonance bands is not practical, confirmation of the chemical kinetic results has been directed toward its detection by rotational and vibrational spectroscopy. Ground-based (3) and balloon-borne (4) measurements of the (J = 11/2 → 9/2) rotational line of ^{35}CℓO at 204.352 GHz have been reported. The balloon-borne detection (5) by infrared vibrational spectroscopy near 12 μm is incorrect (6). Precise laboratory spectroscopy shows that the atmospheric line reported in (5) does not correspond to a transition of CℓO. A subsequent re-examination of the experimental data of Ref. 5 does show the presence of a weak absorption line at the correct frequency to be CℓO (7).

We report here the results of a search for stratospheric CℓO using a ground-based infrared heterodyne spectrometer. Three vibrational lines were searched for near 12 μm, two from the $^2\Pi_{3/2}$ fundamental of ^{35}Cℓ^{16}O and one from the $^2\Pi_{3/2}$ fundamental of ^{37}CℓO. These lines should have been detected if currently accepted abundances are correct, yet none was found. A detailed comparison of the observed and synthetic atmospheric spectra near 856.515 cm^{-1} is reported here. An upper limit to the stratospheric CℓO abundance is derived which is significantly smaller than the abundances obtained from the (independent) chemical kinetic and rotational spectroscopic methods.

Infrared absorption measurements of stratospheric CℓO are important for two reasons: first, because the detection of vibrational absorption lines with the correct frequencies and relative strengths is a necessary condition for the presence of CℓO to be confirmed, and second, because quantitative analysis of the line strengths and shapes provides an independent check on the results obtained by other methods. The vibrational fundamental band (v=0→1) of CℓO lies near 12μm, overlapping both a particularly favorable window in the

terrestrial atmosphere and the $(00^{0}1) - (10^{0}0, 02^{0}0)_{I}$ band of the $^{14}C^{16}O_2$ laser. Close coincidences exist for lines of CℓO (6) with the P8 and P12 transitions of the $^{14}C^{16}O_2$ laser (8), suggesting that detection of stratospheric CℓO by infrared heterodyne spectroscopy (9) using these local oscillator transitions might be possible. Furthermore, recent stratospheric infrared spectra (10), taken at 12.8 air masses and at moderately high resolving power, show weak atmospheric absorption lines with only a few scattered strong lines of tropospheric water vapor in this spectral region. Atmospheric path lengths of this order can readily be obtained from the ground, and strong H_2O lines can be avoided, thus setting the stage for a ground-based search for stratospheric CℓO by ultra-high resolution infrared spectroscopy.

Atmospheric spectra were measured at the Kitt Peak National Observatory ($32^{0}N$, $112^{0}W$) during May and October, 1981, using the McMath Solar Telescope and an infrared heterodyne spectrometer (9) developed at Goddard Space Flight Center. The observing parameters are given in Table 1. The sun was chopped optically against a precision blackbody source (typically 1100 K), and their intensities were adjusted until the mean heterodyne signal (5-1600 MHz) was null-balanced. The difference spectrum was then measured with a 128-channel spectral line receiver. Subsequent measurement of the blackbody reference spectrum, chopped against the room, established the differential transmittance scale and provided an absolute optical calibration for all channels simultaneously.

Each spectrum (9) was recorded at 25 MHz (0.00083 cm^{-1}) resolution with a 64-channel rf filter bank extending 1600 MHz from the laser local oscillator. The spectral region near the expected frequency of the CℓO transition was measured simultaneously over a range of 320 MHz with a second 64-channel filter bank using 5 MHz bandwidth filters. The P12 line at 856.51545 cm^{-1} and the P8 line at 859.78513 cm^{-1} of a line-by-line tuneable $^{14}CO_2$ laser were used as local oscillators in searching for the R9.5 and R12.5 lines of ^{35}CℓO, respectively (Table 1). The R16.5 line of ^{37}CℓO also lies near the P12 line of $^{14}CO_2$, however, it is expected to be only ∿1/3 as strong as the corresponding line of ^{35}CℓO (Table 2). We defer detailed analysis and discussion of the P8 observations to a later paper, except to note that preliminary results based on P8 agree with the results presented here for P12.

A typical spectrum of the measured atmospheric transmittance vs. the

frequency offset from the P12 laser line is shown in Fig. 1. The observed spectrum was acquired on 14 October, 1981, and represents 16 co-added scans (each representing 89 seconds of integration), centered on a time 47 minutes before stratospheric sunset (11) (Table 1). The spectral resolving power ($v/\Delta v$) is 1×10^6 in Fig. 1a and 6×10^6 in Fig. 1b. All channels were acquired simultaneously.

Synthetic atmospheric spectra were calculated for comparison with the measured spectra, including spectral lines of OCS, HNO_3, NO_2,"nano-gen" (see below), and C&O. Since the atmosphere is optically thin in this spectral region, the absorptances were modelled for each molecule individually and later combined linearly, giving the overall atmospheric transmittance to good approximation. A multi-layered spherical atmosphere was constructed, consisting of ten equally thick layers for each species. The layers differed for each species, and were chosen to cover approximately two decades of molecular abundances in each case. Voigt lineshape functions were calculated for each layer using mid-latitude temperature and pressure profiles (12). The modelled spectrum is shown at 25 MHz resolution in Fig. 1a (displaced downward for clarity), and is shown at infinite resolution in Fig. 1b (solid, dashed curves). The model atmosphere used in calculating the synthetic spectra is shown in Fig. 2.

The volume mixing ratio profile used for OCS was the average of the measurements of Mankin et al. (13) and Inn et al. (14) and the modeled profiles of Turco et al. (15) and Sze and Ko (16). Line positions and intensities for OCS were taken from Wells et al. (17) and were also confirmed in the laboratory using the field heterodyne spectrometer. OCS contributes a single line to this spectrum, centered only 25 MHz from the local oscillator (Table 2). Because OCS is tropospheric, this line is strongly pressure broadened and appears in Fig. 1a as a gradually decreasing absorptance as the offset from the local oscillator increases (compare modelled transmittances near 25, 750, and 1400 MHz).

Several features due to stratospheric HNO_3 are seen in Fig. 1a as much narrower absorption lines due to the much lower local pressures. The most obvious HNO_3 absorptions are centered near 156, 554, 963, and 1186 MHz (Table 2). The volume mixing ratio profile used for HNO_3 is the average of the profiles obtained by Barker et al. (18) below about 20 km, and the average of the theoretical profiles summarized by Hudson and Reed (19) above 20 km.

4

Relative intensities and accurate line positions were measured (20) for HNO_3 in the laboratory using a similar heterodyne system.

Stratospheric NO_2 contributes a small amount ($\lesssim 10\%$) to the absorption feature offset 563 MHz from the P12 $^{14}CO_2$ laser line, and it is included in the synthetic spectra. The volume mixing ratio profile used for NO_2 is an average of measurements summarized by Hudson and Reed (19). Line positions for NO_2 were measured in the laboratory (20) using a similar heterodyne system and were found to agree with those given by Flaud et al. (21) to within the experimental error. Ground state energies and absolute line strengths were taken from Flaud et al. (21).

The molecule responsible for the absorption line offset 1500 MHz from the local oscillator frequency has not been identified. This line is not listed on the AFGL trace gas atlas, and our laboratory heterodyne spectroscopy rules out ClO, OCS, HNO_3, H_2O, NO_2, $COCl_2$, Freon-11, Freon-12, CCl_4, CH_3Cl, and C_2H_6 as possibilities for this absorption feature (cf. 20). O_3 is eliminated based on Barbe's results (22). The observed line displays a full-width at half-maximum (FWHM) of $\sim$125 MHz, consistent with a predominantly stratospheric location. Its double side-band depth is $\sim$0.6%, comparable to that of the deepest HNO_3 absorption (near 1186 MHz). It grows with increasing air-mass and is definitely a real, terrestrial atmospheric line. Furthermore, three other (weaker) lines are also present in the observations shown in Fig. 1a, and their widths are consistent with 125 MHz FWHM. These arguments suggest that all four lines are associated with a single molecular species of stratospheric origin with mixing ratio $\sim 10^{-9\pm1}$. We call this constituent "nano-gen" and list the line parameters in Table 2. Fortunately, none of the nano-gen lines falls near the ClO line position.

The absorptance expected for the R9.5 line of ^{35}ClO was calculated using the profile labeled "accepted ClO" in Fig. 2, which represents the mean of nine profiles measured by Anderson and coworkers (2) below about 40 km and the mean of the theoretical profiles summarized by Hudson and Reed (19) above 40 km. The ClO line positions (Table 2) are given by Maki (6) based on diode laser absorption spectroscopy, and were confirmed directly by us using heterodyne spectroscopy in the laboratory. The line strengths (Table 2) are taken from Gillis and Goldman (23), who re-normalized the Boltzmann intensity distribution to the individual line intensities and total band strength measured by Rogowski et al. (24). The pressure broadening coefficient

(4.44±0.23 MHz/Torr at 218K) measured by Pickett et al. (25) for broadening of
$C\ell O$ by N_2 was used.

The modelled spectrum is compared with observations in Fig. 1. The $C\ell O$
lines predicted in the synthetic spectrum are clearly absent in the observed
spectrum measured at both 25 MHz and 5 MHz resolution. Indeed, the 5 MHz
resolution data show dramatically that the accepted stratospheric $C\ell O$
abundances (2-4) are not supported by our infrared data.

Although $C\ell O$ is not detected in our measurements, upper limits on its
stratospheric abundance can be derived. We shall use both subjective and
objective methods to derive upper limits from the 5 MHz resolution data (Fig.
1b). One (subjective) approach is to add gaussian random noise to the
noise-less synthetic spectrum, and then to decrease the $C\ell O$ line depth
proportionally until its presence can just be discerned in the 5 MHz
residuals. This procedure suggests an upper limit which is ~1/5 of the amount
labeled "accepted". We determine an objective upper limit by co-adding
channels symmetrically centered on the line. Abbas et al. (26) have shown
that an optimum signal-to-noise ratio is achieved for gaussian-shaped lines
when the ratio of spectral resolution to full width at half maximum is 1.2.
The FWHM of the expected $C\ell O$ line is 60 MHz, but it departs from gaussian
shape, due to pressure broadening. We thus expect optimum S/N by adding
roughly 15 channels. Co-adding 15 channels, we find the abundance of $C\ell O$
consistent with our data may not exceed 7.1% (1σ) of the "accepted" $C\ell O$
abundance. We shall take 14.2% as an upper limit, the value at the 95%
confidence level (2σ). We thus find the stratospheric $C\ell O$ abundance to be at
least seven times smaller than is currently accepted (Fig. 2). If this were
interpreted as a scaling factor, to be applied to the "accepted" profile, we
would formally derive an upper limit profile as shown in Fig. 2. However, it
must be stressed that our data do not provide any indication that $C\ell O$ is
present anywhere in the stratosphere.

Given our surprisingly small upper limit for $C\ell O$, we must carefully
review possible sources of error. We first consider the effect of
uncertainties in the frequency and the intensity of the R9.5 line of $^{35}C\ell O$.
The frequency of this line is 856.50137±0.00018 cm^{-1} (6). The 5.4 MHz
uncertainty is much less than the width of one of the 25 MHz filters in the
heterodyne spectrometer and should therefore not be a problem at the
resolution used here. Furthermore, we have measured both the R9.5 line of

^{35}ClO and the R16.5 line of ^{37}ClO in a laboratory heterodyne spectrometer identical to the field instrument and find agreement with Maki's values. The intensity used for the R9.5 ClO line is based on the experimentally measured band intensity of 11.8 cm^{-2} atm^{-1} at 296K (23). Margolis et al. (27) have independently measured the band strength to be 13.4 cm^{-2} atm^{-1}. Ab initio calculations of the band strength have been done at the SCF level by Komornicki and Jaffe (28) who find 23 cm^{-2} atm^{-1}. Calculations at the SCF-CI level by Langhoff et al. (29), including the effects of electron correlation, predict a band intensity of 32 cm^{-2} atm^{-1}. A systematic error in the line intensity will certainly affect our results, but there is reason to believe that the experimental line strengths may be too low rather than too high, and this would only make the ClO upper limits even smaller.

According to recent atmospheric models, diurnal variability of ClO does not account for the much lower stratospheric abundances determined from our data. For example, the diurnal model of N. Sze and M. Ko (private communication, 1982) indicates that the integrated ClO column density above 30 km at the time of day corresponding to Fig. 1 is about 85% of the noon-time value, and the diurnal model of J. Herman (private communication, 1982) shows no appreciable change from noon to sunset in the integrated ClO column density above 25 km. It thus seems reasonable to compare our results directly with those obtained near local noon. The mean column density based on nine measurements by the chemical kinetic method (2) is 16.1x10^{13} cm^{-2} and the result using ground-based millimeter-wave spectroscopy (3) is 10.5x10^{13} cm^{-2}. The upper limit reported here using the infrared spectroscopic method is 2.3x10^{13} cm^{-2} at the 95% confidence level, which is considerably smaller than the earlier results. Menzies' (7) latest results also suggest much smaller ClO abundances. We thus find the stratospheric ClO abundance to be at least seven times smaller than currently accepted values, suggesting that the role of ClO and the chlorofluorocarbons in the destruction of the earth's ozone layer may need to be re-evaluated.

Table 1. Observing Parameters During Searches for Stratospheric Chlorine Monoxide.

Date 1981	Local Oscillator	$^{35}Cl O$ Line Searched	Range of Solar Zenith Angle[a]	Range of Stratospheric Air Mass[b]
23 May, Afternoon	P12	R9.5	78.6 - 88.8	4.5 - 10.3
24 May, Morning	P12	R9.5	89.4 - 79.5	10.4 - 4.9
25 May, Morning	P8	R12.5	89.1 - 78.2	10.3 - 4.4
25 May, Afternoon	P8	R12.5	69.6 - 81.8	2.8 - 5.8
14 Oct, Afternoon	P12	R9.5	77.0 - 88.9	4.1 - 10.3
15 Oct, Afternoon	P8	R12.5	75.8 - 88.8	3.8 - 10.2

a. The solar zenith angle is the apparent angle of the sun from the vertical, measured from the ground, and expressed in degrees.

b. The stratospheric air mass is defined to be the ratio of the (refracted) slant-pathlength to the vertical pathlength between two spherical boundaries at 20 and 4 km, as seen by an observer at the ground.

Table 2. Spectral Line Atlas for the 856.5 cm^{-1} Region

Molecule	Frequency (cm^{-1})	Offset[a] (MHz)	S (cm/molecule,296K)[b]
HNO_3[c]	856.5102	156	2.82×10^{-21}
	856.5339	554	1.42×10^{-21}
	856.4970	554	1.42×10^{-21}
	856.4926	685	5.78×10^{-22}
	856.4833	963	2.82×10^{-21}
	856.4759	1186	1.69×10^{-21}
	856.5550	1186	5.00×10^{-21}
	856.5680	1575	1.09×10^{-21}
NO_2[d] $^PP_6$15	856.4967	563	2.36×10^{-22}
OCS[e] P6	856.5146	25	6.24×10^{-21}
^{35}ClO[f] R9.5	856.50137	422	6.99×10^{-21}
^{37}ClO[f] R16.5	856.54146	780	2.16×10^{-21}
Nano-gen[g]		275	0.16%
		688	0.09%
		1038	0.30%
		1500	0.61%

a. Absolute frequency difference relative to the local oscillator transition. Local oscillator is P12 $^{14}CO_2$ at 856.51545 cm^{-1}.

b. These line strength values were scaled to the local temperature for each atmospheric layer in our model atmosphere.

c. Spectroscopic parameters for HNO_3, from Weaver et al. (20).

d. Spectroscopic parameters for NO_2 from Flaud et al. (21).

e. Spectroscopic parameters for OCS from Wells et al. (17).

f. Line position from Maki et al. (6), and line strength from Gillis and Goldman (23).

g. Four lines are observed (see text) Absorptances are given in place of strengths.

REFERENCES

1. F. S. Rowland and M. J. Molina, Rev. Geophys. Space Phys. 13, 1 (1975); C. Miller, D. L. Filkin, A. J. Owens, J. M. Steed, and J. P. Jesson, J. Geophys. Res. 86, 12,039 (1981). For a recent review, see: "Causes and Effects of Stratospheric Ozone Reduction: An Update" (National Research Council (1982), National Academy Press, Washington, DC).

2. J. G. Anderson, H. J. Grassel, R. E. Shetter, and J. J. Margitan, J. Geophys. Res. 85, 2869 (1980). See also E. M. Weinstock, M. J. Phillips, and J. G. Anderson, J. Geophys. Res. 86, 7273 (1981).

3. A. Parrish, R. L. De Zafra, P. M. Solomon, J. W. Barrett, and E. R. Carlson, Science 211, 1158 (1981).

4. J. W. Waters, J. C. Hardy, R. F. Jarnot, and H. M. Pickett, Science 214, 61(1981).

5. (a) R. T. Menzies, Geophys. Res. Letters 6, 151 (1979). (b) R. T. Menzies, C. W. Rutledge, R. A. Zanteson, and D. L. Spears, Appl. Opt. 20, 536 (1981).

6. A. G. Maki, F. J. Lovas, and W. B. Olson, J. Mol. Spectrosc. 92, 410(1982).

7. R. T. Menzies, private communication (1982).

8. C. Freed, L. C. Bradley, and R. G. O'Donnell, IEEE J. Quant. Electronics QE-16, 1195 (1980).

9. M. J. Mumma, T. Kostiuk, and D. Buhl, Opt. Eng. 17, 50 (1978). See also M. J. Mumma, T. Kostiuk, D. Buhl, G. Chin, and D. Zipoy, Opt. Eng. 21, 313 (1982). The relationship between single sideband and double sideband spectra is discussed in these papers.

10. A. Goldman, R. D. Blatherwick, F. H. Murcray, J. W. Van Allen, C. M. Bradford, G. R. Cook, and D. G. Murcray, "New Atlas of IR Solar Spectra" (University of Denver, Denver, 1980).

11. Stratospheric sunset (sunrise) is defined here to be the time of sunset (sunrise) at the point where the line of sight intersects the 30 km altitude shell.

12. "U.S. Standard Atmosphere, 1976", NOAA-S/T 76-1562, U.S. Government Printing Office, Washington, DC, 1976.

13. W. G. Mankin, M. T. Coffey, D. W. T. Griffith, and S. R. Drayson, Geophys. Res. Letters 6, 853 (1979).

14. E. C. Y. Inn, J. F. Vedder, B. J. Tyson, and D. O'Hara, Geophys. Res. Letters 6, 191 (1979).

15. R. P. Turco, R. C. Whitten, O. B. Toon, J. P. Pollack, and P. Hamill, Nature 283, 283 (1980).

16. N. D. Sze and M. K. W. Ko, Nature $\underline{280}$, 308 (1979).

17. J. S. Wells, F. R. Petersen, A. G. Maki, and D. J. Sukle, Appl. Opt. $\underline{20}$, 1676 (1981).

18. D. B. Barker, J. N. Brooks, A. Goldman, J. J. Kosters, D. G. Murcray, F. H. Murcray, J. Van Allen, and W. J. Williams, IEEE Annals No. 75 CH.304-I, 16-6(1976).

19. "The Stratosphere: Present and Future,' Ed. by R. D. Hudson and E. I. Reed (NASA RP 1049, National Aeronautics and Space Administration, Washington, DC 1979).

20. H. Weaver, M. J. Mumma, J. L. Faris, T. Kostiuk, and J. J. Hillman, Appl. Opt. (in press, 1983).

21. J. M. Flaud, C. Camy-Peyret, V. M. Devi, P. P. Das, and K. N. Rao, J. Mol. Spectrosc. $\underline{84}$, 234 (1980). K. N. Rao kindly provided a complete listing of NO_2 line positions and strengths obtained in this work.

22. A. Barbe, private communication, (1981).

23. J. R. Gillis and A. Goldman, J. Quant. Spectrosc. Radiat. Transfer $\underline{26}$, 23 (1981).

24. R. S. Rogowski, C. H. Bair, W. R. Wade, J. M. Hoell, and G. E. Copeland, Appl. Opt. $\underline{17}$, 1301 (1978).

25. H. M. Pickett, D. E. Brinza, and E, A. Cohen, J. Geophys. Res. $\underline{86}$, 7279 (1981).

26. M. M. Abbas, M. J. Mumma, T. Kostiuk, and D. Buhl, Appl. Opt. $\underline{15}$, 427 (1976).

27. J. S. Margolis, R. T. Menzies, and E. D. Hinkley, Appl. Opt. $\underline{17}$, 1680 (1978).

28. A. Komornicki and R. L. Jaffe, J. Chem. Phys. $\underline{71}$, 2150 (1979).

29. S. R. Langhoff, J. P. Dix, J. O. Arnold, R. W. Nicholls, and L. L. Danylewych, J. Chem. Phys. $\underline{67}$, 4306 (1977).

30. J. D. Rogers is an NAS/NRC Resident Research Associate. M. J. Mumma, T. Kostiuk, D. Deming and D. Zipoy were Visiting Astronomers at Kitt Peak National Observatory, which is operated by the Associated Universities for Research in Astronomy, under contract with the National Science Foundation.

Figure Captions

Fig. 1. (a) left. Observed and modelled spectra of the terrestrial atmosphere near the P12 $^{14}CO_2$ laser line. The frequency resolution is 25 MHz and the spectra are displayed as transmittance vs. the frequency difference from 856.515 cm^{-1}. The modelled spectrum is displaced downward for clarity, and the expected line of $^{35}C\ell O$ is indicated. The atmospheric model is described in the text.

Fig. 1. (b) right. Observed and modelled spectrum, centered on the R9.5 $C\ell O$ line. The frequency resolution in the observed spectrum is 5 MHz and the modelled spectrum is displayed with infinite resolution. The residual differences between the observations and the modelled spectrum without $C\ell O$ are shown, and are compared with the expected $C\ell O$ line.

Fig. 2. Volume mixing ratio profiles for OCS, HNO_3, NO_2 and $C\ell O$ used in simulating the experimental spectra. The three measurements on $C\ell O$ indicated by the crosses are from Waters et al. (4). See text for a discussion of the profiles. The dashed profile represents an upper limit to a stratospheric $C\ell O$ abundance profile consistent with the infrared data.
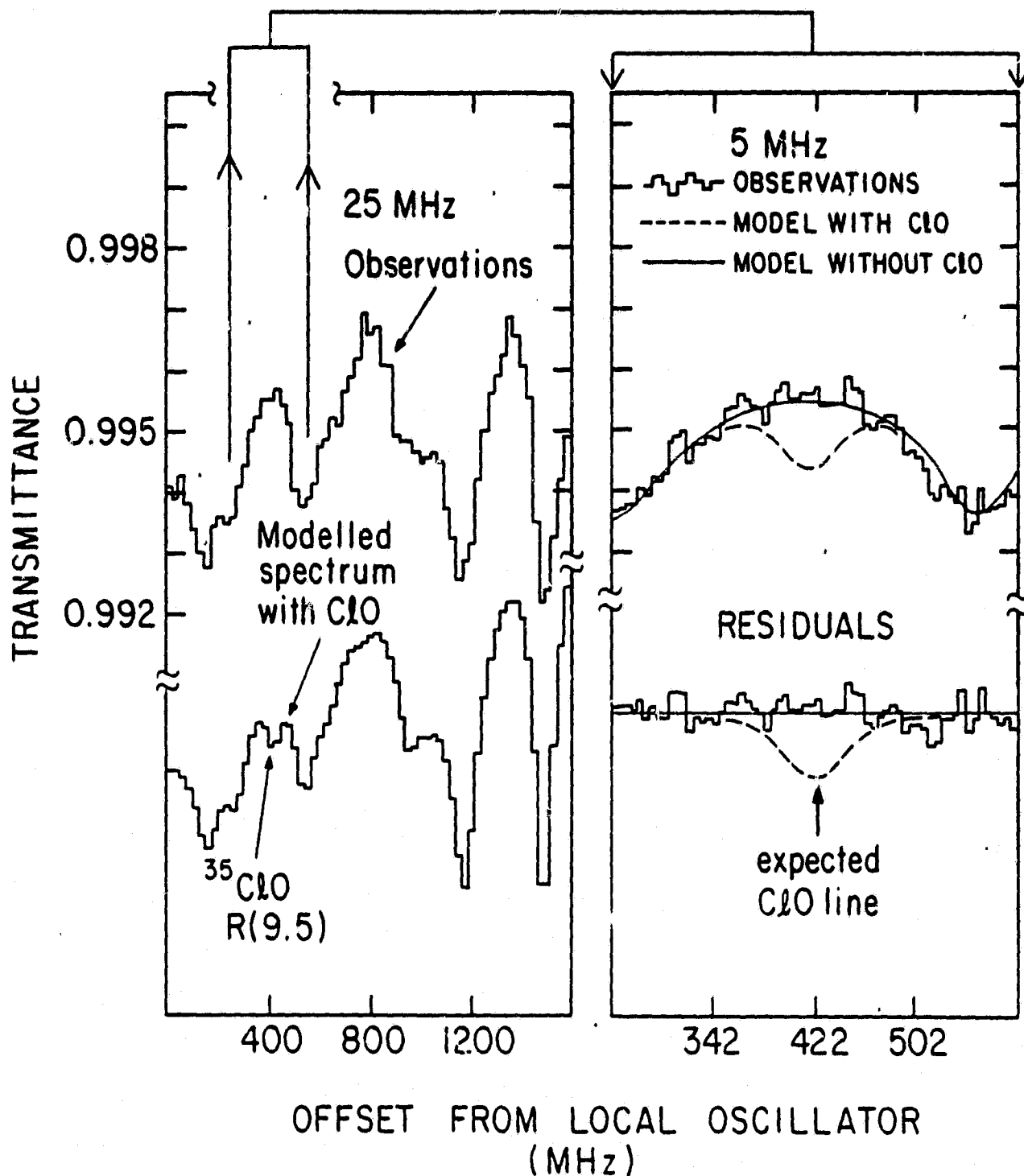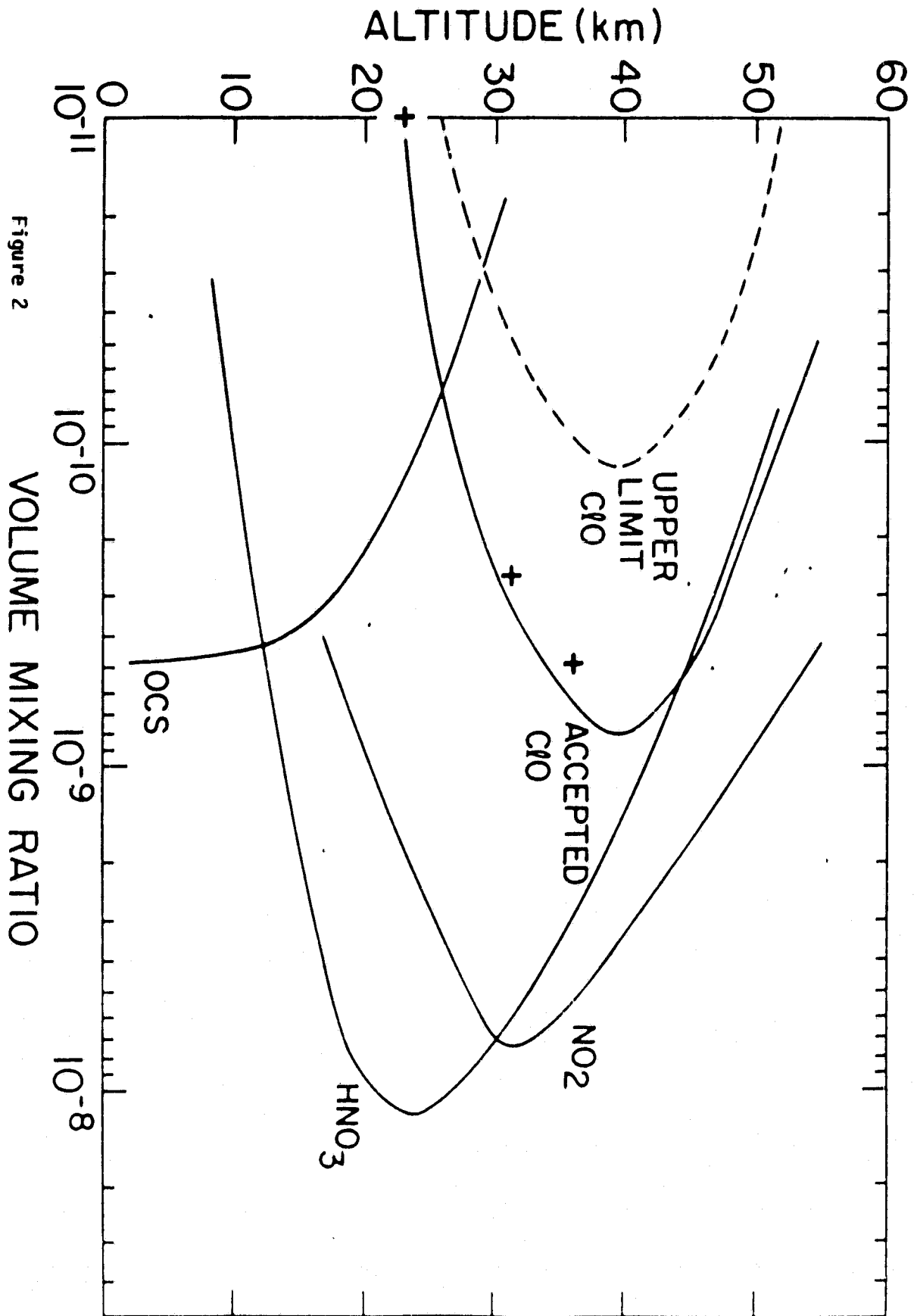
OFFSET FROM LOCAL OSCILLATOR
(MHz)

Figure 1

Figure 2